AN_EXTENDED_VALIDATION_OF .pdf

by

Submission date: 12-Jul-2021 06:29PM (UTC+0700)
Submission ID: 1618674467
File name: AN_EXTENDED_VALIDATION_OF.pdf (958.13K)
Word count: 6736
Character count: 33678

33

AN EXTENDED VALIDATION OF FREEFOAM APPLICATION TO SHIP RESISTANCE PREDICTION FOR USING IN PRELIMINARY DESIGN STAGE

BASCO A. ARDIANTO, OSMAN A. DJE ANGGRIANI
22

7
7
6
18

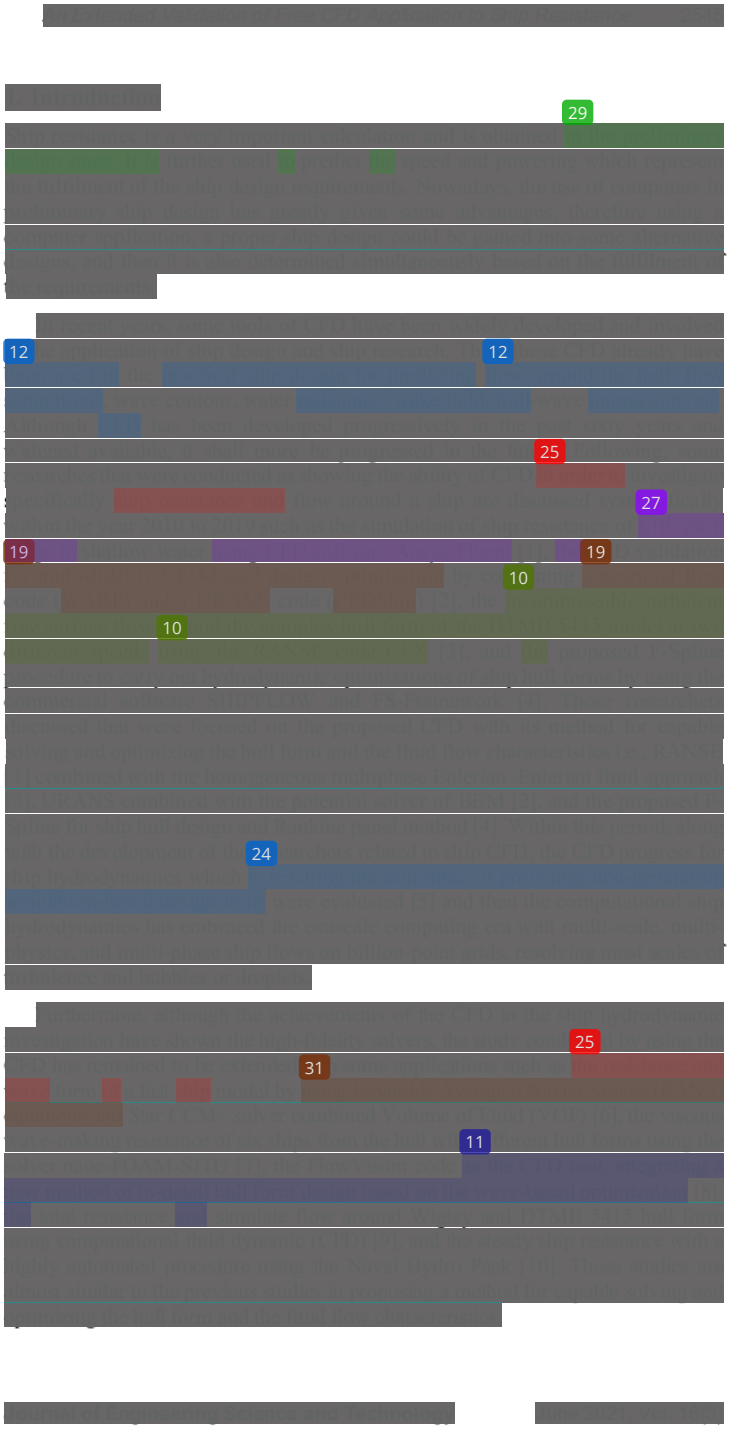

[redacted]

[redacted]

[redacted]

[redacted]

[redacted]

2. Computational Methods

2.1. Overview of Autodesk CFD

The finite element method (FEM) can be used in the fluid dynamic application with special techniques for a conservative solution. The FEM is much more stable compared with the other discretization methods. In Autodesk CFD [21, 22], the FEM is used to reduce the governing partial differential equations (PDES) to a set of algebraic equations. In this method, the dependent variables are represented by polynomial shape functions over a small area or volume (element). Then, the FEM is a particular numerical method for solving partial differential equations in two or three space variables and to predict the behaviour of each element. The result is a set of algebraic equations for the dependent variable at discrete points or nodes on every element. Correspondingly, a real object into a large number of finite elements is analysed by using, a type of computerized analysis method, the finite element analysis (FEA). Autodesk CFD uses FEM primarily because of its flexibility in modelling any geometric shape such as linear for 3D tetrahedral elements (unstructured grids) wherein Galerkin's method of weighted residuals is generally used. Hence, the geometric flexibility inherent in finite elements has been maintained in Autodesk CFD.

2.2. Governing equations

The governing equations for fluid flow are the external incompressible flow of the Navier-Stokes or momentum equations [22]. The governing PDES for continuity equation can be written as:

$$\frac{\partial \rho}{\partial t}+\frac{\partial \rho u}{\partial x}+\frac{\partial \rho v}{\partial y}+\frac{\partial \rho w}{\partial z}=0 \tag{1}$$

where, ρ is the density, t is the time, u is the velocity component in x-direction, v is the velocity component in y-direction, and w is the velocity component in z-direction.

Then, X-Momentum, Y-Momentum, and Z-Momentum equations are derived from the continuity equation as follows. X-Momentum is given:

$$\rho\frac{\partial u}{\partial t}+\rho u\frac{\partial u}{\partial x}+\rho v\frac{\partial u}{\partial y}+\rho w\frac{\partial u}{\partial z}$$
$$=\rho g_x-\frac{\partial p}{\partial t}+\frac{\partial}{\partial x}\left[2\mu\frac{\partial u}{\partial x}\right]+\frac{\partial}{\partial y}\left[\mu\left(\frac{\partial u}{\partial y}+\frac{\partial v}{\partial x}\right)\right]$$
$$+\frac{\partial}{\partial z}\left[\mu\left(\frac{\partial u}{\partial z}+\frac{\partial w}{\partial x}\right)\right]+S_\omega+S_{DR} \tag{2}$$

Y-Momentum equation is given:

$$\rho\frac{\partial v}{\partial t}+\rho u\frac{\partial v}{\partial x}+\rho v\frac{\partial v}{\partial y}+\rho w\frac{\partial v}{\partial z}$$
$$=\rho g_y-\frac{\partial p}{\partial y}+\frac{\partial}{\partial x}\left[\mu\left(\frac{\partial u}{\partial y}+\frac{\partial v}{\partial x}\right)\right]+\frac{\partial}{\partial y}\left[2\mu\frac{\partial v}{\partial y}\right]$$
$$+\frac{\partial}{\partial z}\left[\mu\left(\frac{\partial v}{\partial z}+\frac{\partial w}{\partial y}\right)\right]+S_\omega+S_{DR} \tag{3}$$

Z-Momentum equation is given:

$$\frac{\partial w}{\partial t}+\rho u\frac{\partial w}{\partial x}+\rho v\frac{\partial w}{\partial y}+\rho w\frac{\partial w}{\partial z}=\rho g_z-\frac{\partial p}{\partial z}+\frac{\partial}{\partial x}\left[\mu\left(\frac{\partial u}{\partial z}+\frac{\partial w}{\partial x}\right)\right]+\frac{\partial}{\partial y}\left[\mu\left(\frac{\partial v}{\partial z}+\frac{\partial w}{\partial y}\right)\right]+\frac{\partial}{\partial z}\left[2\mu\frac{\partial w}{\partial z}\right]+S_\omega+S_{DR} \quad (4)$$

where, g_x, g_y, g_z are the gravitational acceleration in x, y, z directions, μ is the viscosity, S_ω rotating flow, and S_{DR} is the distributed resistance term.

The two source terms in the momentum equations are $S\omega$ for rotating coordinates and S_{DR} distributed resistances, respectively. The distributed resistance term can be written in general as:

$$\boldsymbol{S_{DR}=-\left(K_i+\frac{f}{D_H}\right)\frac{\rho V_i^2}{2}-C\mu V_i} \quad (5)$$

where, V is the velocity, i refers to the global coordinate direction (u, v, w momentum equation), f is the friction factor, d is the hydraulic diameter, C is the permeability. K-factor term can operate on a single momentum equation at a time because each direction has its own unique K-factor. The other two resistance types operate equally on each momentum equation.

The other source term is for rotating flow. This term can be written in general as:

$$S_\omega=-2\,\rho\omega_i\times V_i-\rho\omega_i\times\omega_i\times r_i \quad (6)$$

where, ω is the rotational speed and r is the distance from the axis of rotation.

For turbulence models, this study uses the wall function or *k-epsilon* (k-ε), k is the kinetic energy per unit mass and ε is the turbulent dissipation wherein it is suitable for the interactions of the external incompressible flow with complex geometry.

3. Computational Conditions

3.1. Ship data and model scale

The actual ship which was employed in this simulation is a general cargo type. There are two ship models in this simulation namely the model with a bulbous bow (BB) and without a bulbous bow (WBB). The principal particulars of the actual ship and the scaled models are provided in Table 1. The ship model scale is 1:40. The body plan of the actual ship is shown in Fig. 1.

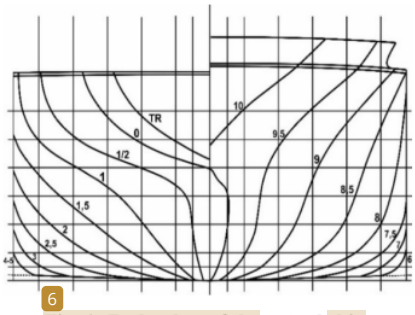

Fig. 1. Body plan of the actual ship.

3.2. Computational domain, boundary and mesh sizing conditions

For ship resistance test, the computational domain of a water tank is a rectangular block and a tetrahedral mesh as shown in Fig. 2, and then in this study, the size of the computational domain was considered the boundary conditions and the area of the flow directions to the free cross-section between the fluid region and solid region. Therefore, the size of the computational domain was decided sufficient large and matched the blockage correction of the width and depth between ship model and water tank for the ship resistance test wherein the size of the length is 4.57 *Lbp*, width is 2 *Lbp*, and depth 1 *Lbp* as defined in *x, y*, and *z*-directions, respectively. The fluid flow points *x*-direction, *y*-direction is the port-starboard of the flow direction, and the positive *z*-axis is upward. For the boundary conditions, the upstream inlet and far-field boundary were specified for velocity and turbulent properties and the reference pressure was applied downstream. A slip boundary was applied on the top, *Y*-min, and *Y*-max boundary. The boundary conditions in the computational domain are shown in Fig. 2. The material of the ship model was input as a solid (steel) phase and the water tank was liquid (seawater) phase.

Table 1. Principal particulars of ship and models.

Description	Actual Ship	WBB	BB
Length over all/*Loa* (m)	73.3	1.83	1.83
Length between perpendiculars/*Lbp* (m)	70.1	1.75	1.75
Breadth/*B* (m)	11.5	0.29	0.29
Draught/*D* (m)	7.0	0.18	0.18
Draft/*d* (m)	5.5	0.14	0.14
Wetted surface area (m^2)	1312.83	0.805	0.817

In this study, in order to obtain a high accuracy of the computational results, the box region was considered to build around the ship model for adding a fine mesh. The mesh size of the box region is suited with the solid mesh. By using the box region, the initial input and computational condition do not change during the simulation process.

On the other hand, the adequate number of meshes in order to ensure the accuracy of computation results also was examined by using the comparison result between the Autodesk CFD and experimental results at water velocity 0.894 m/sec or Froude number (*Fr*) 0.213 for both model BB and WBB as shown in Tables 2 and 3, respectively. For model BB, case 3 which gives the small deviation was selected wherein the total mesh number of the fluid element is 8228836 and the solid element of the model BB is 1325809. Meanwhile, case 3 also was selected for the model WBB wherein the mesh number of the fluid and solid elements are 4277049 and 107820, respectively. The ship model meshing for both model BB and WBB is shown in Fig. 3.

In the Autodesk CFD, the convergence criteria by the ratio of the residual out and residual are given 1.0E-08 for ensuring the stability and convergence of the analysis. In this study, the convergence of the pressure parameter was examined in the iteration of the simulation 300, and then the ratio of the residual in and residual out was obtained 4.22E-12 for BB simulation at *Fr* 0.213 and 1.70E-12 for WBB simulation at *Fr* 0.213. This means that the presence of computational simulation is stable.

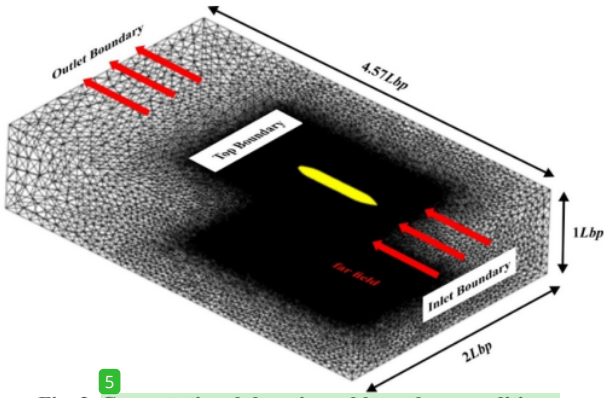

Fig. 2. Computational domain and boundary conditions.

(a) Model BB meshing.

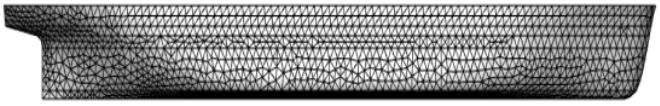

(b) Model WBB meshing.

Fig. 3. Ship model meshing.

Table 2. The mesh number of the BB simulation.

Case	Element	Mesh number	*Fr*	CFD	Exp.	Dev. (%)
1	Fluid element Solid element	824121 4725	0.213	2.618	2.393	8.59
2	Fluid element Solid element	821031 4748	0.213	2.594	2.393	7.75
3	Fluid element Solid element	8228836 1325809	0.213	2.516	2.393	4.89

Table 3. The mesh number of the WBB simulation.

Case	Element	Mesh number	*Fr*	CFD	Exp.	Dev. (%)
1	Fluid element Solid element	839354 4573	0.213	3.142	2.586	17.70
2	Fluid element Solid element	4222022 17876	0.213	2.769	2.586	6.61
3	Fluid element Solid element	4277049 107820	0.213	2.717	2.586	4.82

4. Results and Discussion

4.1. Computational results

The CFD simulations by using Autodesk CFD were successfully carried out by using some techniques as discussed in the section on the computational conditions and then the results are discussed accordingly. In this simulation, the fluid flow was in a steady-state and then turbulent flow was applied. The iteration number was 300 per model's velocity. In addition, the computational simulations were run in the increasing of the water velocity as assumed equal to the model's velocity from 0.081 m/sec to 0.894 m/sec or Froude number (Fr) 0.019 to 0.213. The maximum *Fr* set in the computational simulation was considered in the same maximum Fr of the actual ship.

4.1.1. Fluid velocity, pressure distribution, and vortex generation

The velocity field around WBB and BB has been captured within the box region on centre plane y = 1.0 *Lbp* as visualized in Fig. 4 wherein the initial input of the water velocity was set at 0.894 m/sec or *Fr* 0.213.

The contour of the water velocity magnitude around BB and WBB is coded by the different colour (brightness). The flow velocity gradually decreases after hitting the bow part for both model BB and WBB. The boundary of the flow velocity around BB is different from WBB especially in the bottom and rear part wherein the velocity magnitude around BB is lower than WBB. This different magnitude impacts wake along with the model a[5] pressure distribution along the model's body. Therefore, the effect of bow shape influences the flow velocity around the model.

The effect of the flow velocity around the mode[6]n pressure distribution acting on BB and WBB surface has been captured as shown in Fig. 5. The pressure distribution acts dominantly high on the bow region for both model BB and WBB at *Fr* 0.213. The range of the pressure coefficient shows the difference between model BB and WBB wherein the positive pressure coefficient of the model BB is higher than WBB whereas the negative pressure coefficient of the model WBB is lower than BB.

The peak pressure coefficient of the model BB is 1.073 and the lower pressure coefficient is -0.314. Meanwhile, for the model WBB, the peak pressure coefficient is 0.917 and the lower pressure coefficient is -0.416. The negative pressure coefficients act on the surface of the bow shoulder for both model BB and WBB. Also, the negative pressure impacts the bow shoulder region of both models, and this negative pressure can decrease the viscous pressure resistance.

On the other side, the inflow was driven by the forebody downstream and the flow momentum on the aft body generates a big vortex contour. The occurrence of the big contour shows the difference between model BB and WBB at *Fr* 0.213 as shown in Fig. 6. In the case of the BB, the wake occurs on the region of the bow shoulder to the mid-body as shown in Fig. 6(a) whereas it occurs behind the mid-body to the stern region as shown in Fig. 6(b).

The overall hydrodynamic parameters such as water velocity, pressure distribution, and vorticity that were obtained by using Autodesk CFD increase in the increasing *Fr* for both models WBB and BB.

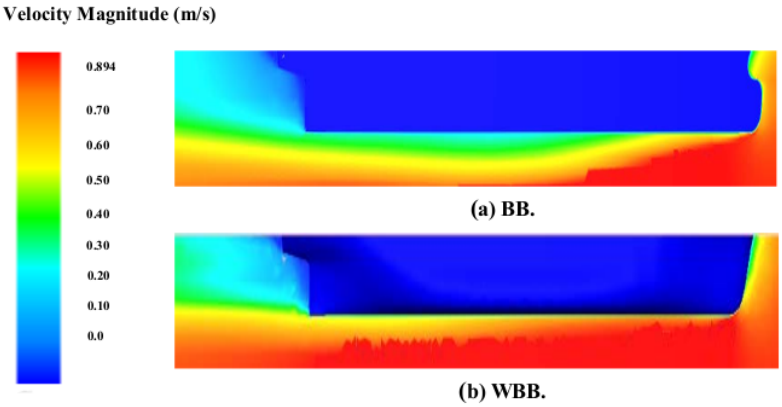

(a) BB.

(b) WBB.

Fig. 4. Velocity magnitude at Fr 0.213.

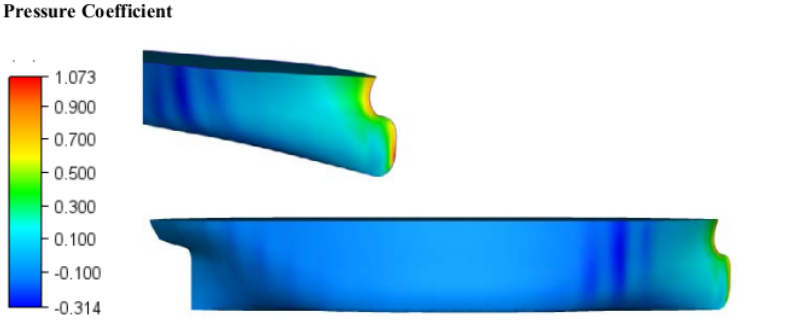

(a) BB.

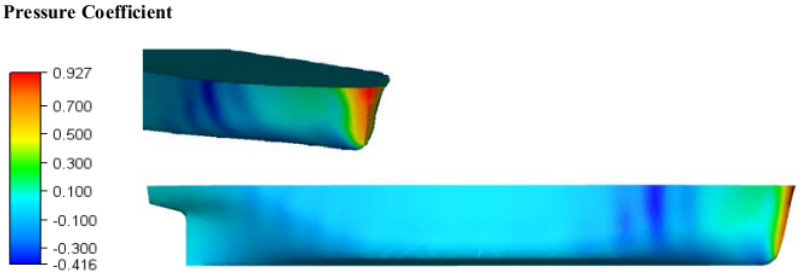

(b) WBB.

Fig. 5. Pressure distribution on hull surface at *Fr* 0.213.

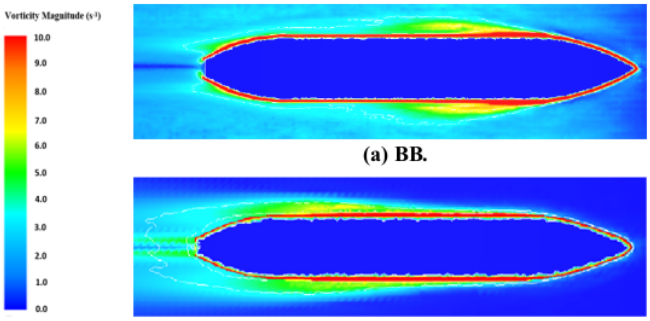

(a) BB.

(b) WBB.

Fig. 6. The vortex generation in flow field at *Fr* 0.213.

4.1.2. Ship resistance

Ship water resistance, as a total resistance (*Rt*), was predicted successfully and then the comparison of the water resistance between model BB and WBB was obtained as well. Figure 7 shows the tendency of water resistance coefficient in both model BB and WBB in the increasing of the *Fr* from 0.019 to 0.213. The coefficient of water resistance (*Ct*) is defined by *Rt/0.5ρSV2* wherein *S* is the wetted area and *V* is the model's velocity. This can be seen that the water resistance coefficient tends to decrease in the increasing of the *Fr* and the tendency of the water resistance coefficient for both model BB and WBB is similar. The coefficient of water resistance of the model WBB is higher than the model BB and the difference value of the water resistance coefficient is obtained 13.58%.

Although both models have the same geometric parameter of the length to beam ratio and a small difference only the shape of the bow part, this Autodesk CFD application can distinguish the effect of the bulbous bow on the magnitude of viscous pressure drag as given the different value such the obtained coefficient of the water resistance *Ct*. The causes of this difference have been also depicted clearly by Figs. 4 to 6.

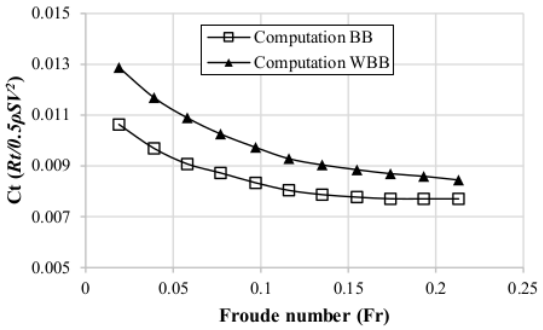

Fig. 7. The tendency of water resistance coefficient (*Ct*) in increasing *Fr*.

The physical time spent in this computational simulation was approximately 3.77 hours per case for model WBB and then 10.32 hours per case for model BB. The specifications of the laptop which was used in this study are Intel i7-8550U @ 1.99 GHz, RAM 16 GB, 64-bit operating system, and x64-based processor. Based on the time cost and laptop specifications, the investigation of ship resistance, pressure distribution, and vortex flow can be carried out by using the Autodesk CFD in the preliminary ship design stage. In the future study, a free surface flow along ship and other flow phenomena due to high speed will be conducted by using the transient analysis.

4.2. Experimental results

The experiments of both model BB and WBB on pressure distribution, wave profile, and water resistance were successfully conducted in Towing Tank, Ship Hydrodynamics Laboratory, Naval Architecture Department, Engineering Faculty, Hasanuddin University. The towing tank sizes are 60 m in length, 4 m in width, and 4 m in depth. Before using this new towing tank, the resistance of the same model is benchmarked conducted by the other towing tank. The speed of the towing carriage is a maximum of 4 m/sec. In the experimental works, the models had the same main dimensions as the computational models and several model's speeds were considered namely 0.244 m/sec (*Fr* 0.058), 0.488 m/sec (*Fr* 0.116), 0.732 m/sec (*Fr* 0.174), and 0.894 m/sec (*Fr* 0.213) as well those representative speeds, described the speed increase, could provide sufficient data to be used for validating the computational results. For the effects of a boundary due to the water flow around the model, the blockage effect was corrected by using *B*model <*B*tank/10 to *B*tank/15 and *d*model <*h*tank/10 to *h*tank/20. The value of the blockage met with the correction range and was considered in this experimental work. Moreover, for the resistance experiment, the model was provided without the attachments of the piezoelectric device and its installations.

4.2.1. Pressure distribution

The pressure distributions that are acting on the model surface under water level were investigated experimentally with various Froude numbers. Figure 8 shows piezoelectric sensors which were attached and installed on both model surface BB and WBB. The piezoelectric sensor is connected to breadboard and Arduino mega and then these were installed to the computer as shown the block diagram in Fig. 9.

Figure 10 shows the examples of time history pressure distributions that are measured on *P1*, *P2*, *P3* and *P4* on the bow part of the model BB and WBB respectively at *Fr* 0.213. The time history of the pressure distributions was recorded in ten seconds. The average of the peak pressure acting on bow part BB are obtained *P1* 421.753 (N/m^2), *P2* 419.231 (N/m^2), *P3* 411.774 (N/m^2), and *P4* 378.710 (N/m^2) and then the average of the overall peak pressure magnitude *P1*, *P2*, *P3*, and *P4* are obtained 407.867 (N/m^2). For the peak pressure on the bow part, the average of the peak pressure is *P1* 506.584 (N/m^2), *P2* 470.754 (N/m^2), *P3* 210.933 (N/m^2), and *P4* 215.377 (N/m^2) and then the average of the overall peak pressure magnitude *P1*, *P2*, *P3*, and *P4* are obtained 350.912 (N/m^2). For the comparison of the average of the overall peak pressure acting on the bow part, the model BB is higher than model WBB and the difference is around 13.96%. Meanwhile, the average of the peak pressure on the stern part BB is obtained *P9* 46.706 (N/m^2), *P10* 113.073 (N/m^2),

P11 61.598 (N/m^2), and *P12* 61.598 (N/m^2) and then the average of the overall peak pressure is 70.744 (N/m^2).

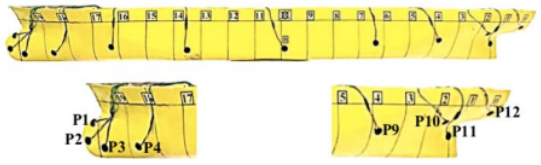

(a) BB.

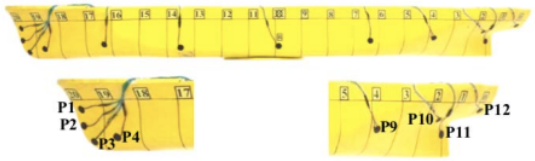

(b) WBB.

Fig. 8. The ship model with the attached piezoelectric.

Moreover, the average of the pressure distributions on the stern part WBB is *P9* 61.045 (N/m^2), *P10* 115.073 (N/m^2), *P11* 71.369 (N/m^2), and *P12* 72.428 (N/m^2) and then the average of the overall peak pressure is 79.978 (N/m^2). The average peak pressure of the model WBB is higher than model BB and it has a different value of approximately 11.55%. Although the peak pressure on bow part BB is sufficiently higher than WBB, in contrast, the peak pressure on stern part WBB is higher. As a result of higher peak pressure due to bulbous bow shape compared without the bulbous bow, this can be noted that the effect of the bulbous bow could reduce water pressure along the model's body and water intake (vortex field) after passing the bow part.

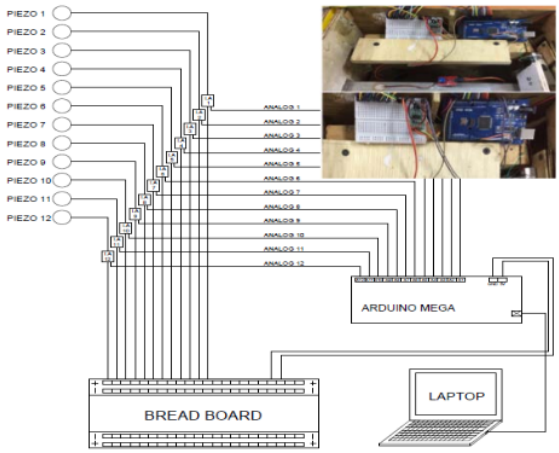

Fig. 9. Block diagram of piezoelectric sensor installation.

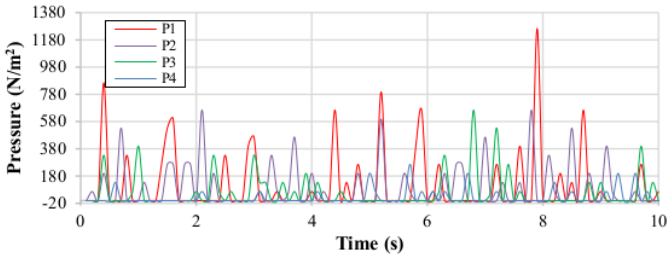

(a) BB.

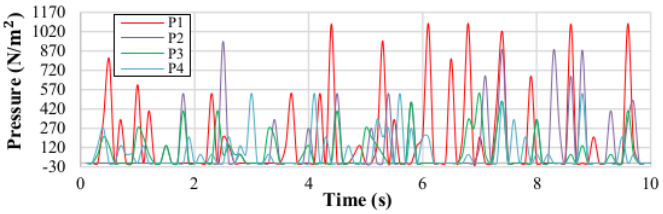

(b) WBB.

Fig. 10. Time history of pressure distribution on bow part at *Fr* 0.213.

Here, the pressure coefficient *Cp* is defined by *Pmax*/0.5ρ*V2* wherein *Pmax* is peak pressure, ρ is water density, and *V* is water velocity. The peak pressure coefficient of the model BB is obtained 1.021 and for WBB it is obtained 0.878. For the comparison of the peak pressure coefficient on the bow part between the Autodesk CFD as shown in Fig. 5 and experimental result, the *Cp* of the model BB and WBB as resulted by the Autodesk CFD is higher than the experimental results and the difference is obtained around 4.88% and 5.23% respectively. Meanwhile, the *Cp* of the experiment result for BB and WBB on the stern part is 0.177 and 0.200, respectively. Those experimental *Cp* are in the range of the computational *Cp*. Therefore, the computational *Cp* of the model BB and WBB shows good agreement with the experimental result.

4.2.2. Ship resistance

Ship resistance of both model BB and WBB was carried out successfully by performing experiments in various increasing the *Fr* in 0.058, 0.116, 0.174, and 0.213. Figure 11 shows the model BB and WBB that were used in the experiment. Figure 12 shows the tendency of the water resistance coefficient *Ct* for the model BB and WBB between computational and experimental results. The tendency of the *Ct* between computational and experimental results shows similar as well the *Ct* of the computational results for both models are higher than the experimental results. For small *Fr* ($\leq$ 0.075), the *Ct* between the experimental and computational result for model BB and WBB has a very small difference.

(a) BB.

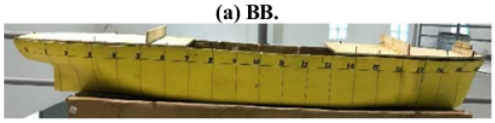

(b) WBB.

Fig. 11. Ship models for towing tank experiment.

The different value of the *Ct* between the computational and experimental result at *Fr* 0.058, 0.116, 0.174, and 0.213 for model BB is obtained 3.59% and then for model WBB, the different value is obtained 4.86%. Therefore, the overall computational water resistance coefficient *Ct* confirms good agreement with the experimental result.

Based on the time cost and laptop specifications for the computational simulation that have been discussed previously, the computational results of the ship resistance, pressure distribution has been validated with experimental results and then by the validation results, this adds an adequate reason for using widely the Autodesk CFD in the preliminary ship design stage.

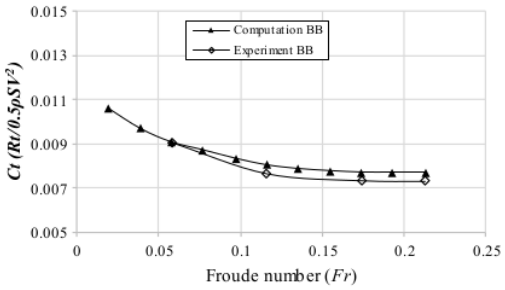

(a) BB.

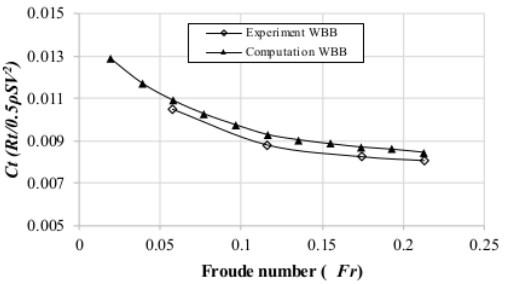

(b) WBB.

Fig. 12. The tendency of water resistance coefficient.

5. Conclusions

Herein the predictions of ship hydrodynamics by using the free application of Autodesk CFD were successfully conducted and then the dynamic parameters such as the velocity magnitude around the ship, pressure distribution on the ship hull, vortex field, and water resistance were obtained.

Correspondingly, the experimental works were carried out successfully as well to validate the obtained results of the free Autodesk CFD application. The comparisons of the coefficient peak pressure *Cp* on bow surface BB and WBB between the experimental and computational results are obtained the different magnitude around 4.88% and 5.23% respectively whereas the *Cp* of the computational result on stern part BB and WBB are in the same range magnitude with the experimental results. These *Cp* comparisons show good agreement.

Moreover, the computational results of the water resistance coefficient *Ct* in the increasing *Fr* have a similar tendency with the experimental results for both model BB and WBB. The different value of the *Ct* between the computational and experimental result at *Fr* 0.058, 0.116, 0.174, and 0.213 for model BB is obtained 3.59% and then for model WBB, the different value is obtained 4.40%. Therefore, the overall computational water resistance coefficient *Ct* confirms good agreement with the experimental result.

Based on the overall results above, the free Autodesk CFD application could be used practically in the preliminary ship design stage. In addition, a computer or laptop which is used for the computational simulation is recommended minimum specifications. In the future study, a free water surface along with the ship and other flow phenomena will be investigated by using the transient flow analysis provided by Autodesk CFD.

Acknowledgements

The authors would like to thank gratefully Ahmad Amsal Rasidi, Aji Prayoga, Rafika Arifin, Yance Mangalla, Muhammad Fadel Ramadhan and Abdul Wahid Hasim for their useful helps in conducting the computational simulation and experimental work.

Nomenclatures

C	Permeability
C_p	Pressure coefficient
Ct	Water resistance coefficient
f	Friction factor
Fr	Froude number
gx	Gravitational acceleration in x-direction
gy	Gravitational acceleration in y-direction
gz	Gravitational acceleration in z-direction
k	Kinetic energy
K_i	K-factor term
q_V	Volumetric heat source
r_i	Distance from the axis of rotation
Rt	Total Resistance
S_{DR}	Distributed resistance term

S_ω	Rotating flow
t	Time, s
	Total temperature
u	Velocity of flow in x-direction
v	Velocity of flow in y-direct
V_i	Velocity global coordinate direction
w	Velocity of flow in z-direction

Greek Symbols

ρ	Density
μ	Viscosity
ω	Rotational speed
Φ	Dissipation function
ε	Turbulent dissipation

Abbreviations

BB	Bulbous Bow
CFD	mputational Fluid Dynamics
FEM	Finite Element Method
FEA	Finite Element Analysis
FVM	Finite Volume Method
ITTC	International Towing Tank Conference
Lbp	Length between perpendicular
Loa	Length over a
OpenFOAM	Open-source Field Operation and Manipulation
PDES	Partial Differential Equations
RANS	Reynolds Averaged Navier Stokes
VOF	Volume of Fluid
WBB	Without Bulbous Bow

References

1. Benes, P.; and Kollarik, R. (2011). Preliminary computational fluid dynamics (CFD) simulation of EIIb push barge in shallow water. *Scientific Proceedings Faculty of Mechanical Engineering*, 19(1), 67-73.
2. Kandasamy, M.; Ooi, S.K.; Carrica, P.; Stern, F.; Campana, E.F.; Peri, D.; Osborne, P.; Cote, J.; Macdonald, N.; and Waal, N. (2011). CFD validation studies for a high-speed foil-assisted semi-planning catamaran. *Journal of Marine Science and Technology*, 16(2), 157-167.
3. Ahmed, Y.M. (2011). Numerical simulation for the free surface flow around a complex ship hull form at different Froude numbers. *Alexandria Engineering Journal*, 50(3), 229-235.
4. Han, S.; Lee, Y.-S.; and Choi, Y.B. (2012). Hydrodynamic hull form optimization using parametric models. *Journal of Marine Science and Technology*, 17, 1-17.
5. Stern, F.; Yang, J.; Wang, Z.; Sadat-Hosseini, H.; Mousaviraad, M.; Bhushan, S.; and Xing, T. (2013). Computational ship hydrodynamics: Nowadays and way forward. *International Shipbuilding Progress*, 60(1-4), 3-105.

6. Ozdemir, Y.H.; Barlas, B.; Yilmaz, T.; and Bayraktar, S. (2014). Numerical and experimental study of turbulent free surface flow for a fast ship model. *Brodogradnja/Shipbuilding*, 65(1), 39-54.
7. Zha, R.; Ye, H.; Shen, Z.; and Wan, D. (2014). Numerical study of viscous wave-making resistance of ship navigation in still water. *Journal of Marine Science and Application*, 13, 158-166.
8. Aksenov, A.A.; Pechenyuk, A.V.; and Vucinic, D. (2015). *Towards green marine technology and transport* (1st ed.). Chapter: Ship hull form design and optimization based on CFD. CRC Press, 215-223.
9. Ahmed, Y.M.; Yaakob, O.B.; Rashid, M.F.A.; and Elbatran, A.H. (2015). Determining ship resistance using computational fluid dynamics (CFD). *Journal of Transport System Engineering*, 2(1), 20-25.
10. Gatin, I.; Vukčević, V.; Škurić, V.; and Jasak, H. (2018). *Technology and science for the ships of the future*. Chapter: Fully automated ship resistance prediction using the naval hydro pack. IOS Press, 256-263.
11. Park, S.; Park, S.W.; Rhee, S.H.; Lee, S.B.; Choi J.-E.; and Kang, S.H. (2013). Investigation on the wall function implementation for the prediction of ship resistance. *International Journal of Naval Architecture and Ocean Engineering*, 5(1), 33-46.
12. Jasak, H.; Vukcevic, V.; and Christ, D. (2014). Rapid free surface simulation for steady-state hull resistance with FVM using OpenFOAM. *Proceedings of the 30th Symposium on Naval Hydrodynamics*. Tasmania, Australia, 1-7.
13. Axner, L.; Gong, J.; Chiarini, A.; and Mascellaro, L. (2014). SHAPE pilot monotricat SRL: Hull resistance simulations for an innovative hull using OpenFOAM. *Partnership for Advanced Computing in Europe*, 1-8.
14. Wang, J.; and Wan, D. (2017). Breaking wave simulations of high-speed surface combatant using OpenFOAM. *Proceedings of the 8th International Conference on Computational Methods*. Guangxi, China, 841-852.
15. Rahaman, M.M.; Islam, H.; Islam, M.T.; and Khondoker, M.R.H. (2017). Calm water resistance prediction of a bulk carrier using Reynolds averaged Navier-Stokes based solver. *AIP Conference Proceedings*, 1919(1), 1-6.
16. Kim, G.-H.; and Park, S. (2017). Development of a numerical tool for efficient and robust prediction of ship resistance. *International Journal of Naval Architecture and Ocean Engineering*, 9(5), 537-551.
17. Bustos, D.S.H.; and Alvarado, R.J.P. (2017). Numerical hull resistance calculation of a catamaran using OpenFOAM. *Ship Science and Technology*, 11(21), 29-39.
18. Islam, H.; and Soares, C.G. (2017). *Maritime transportation and harvesting of sea resources*. Chapter: Prediction of ship resistance in head waves using OpenFOAM. Taylor and Francis Group, 527-533.
19. ITTC. (2014). Practical guidelines for ship CFD applications (No. 7.5-03-0203). Retrieved August 21, 2019, from https://ittc.info/media/1357/75-03-02-03.pdf.
20. ITTC. (2014). Practical guidelines for ship resistance CFD (No. 7.5-03-0204). Retrieved August 21, 2019, from https://ittc.info/media/4198/75-03-02-04.pdf.

21. Autodesk CFD. (2017). Inventor: System requirements for Autodesk inventor 2017 products. Retrieved August 21, 2019, from https://www.autodesk.com/education/free-software/inventor-professional.
22. Autodesk CFD. (2017). Learning guide: General fluid flow and heat transfer equations. Retrieved August 21, 2019, from https://knowledge.autodesk.com/support/cfd/learn-explore/caas/CloudHelp/cloudhelp/2017/ENU/SimCFD-Learning/files/GUID-83A92AE5-0E9E-4E2D-B61F-64B3696E5F66-htm.html.

AN_EXTENDED_VALIDATION_OF.pdf

ORIGINALITY REPORT

15%	%	15%	%
SIMILARITY INDEX	INTERNET SOURCES	PUBLICATIONS	STUDENT PAPERS

PRIMARY SOURCES

1	Janaka Wijekoon, Divya Amunugama, Hiroaki Nishi. "On the effectiveness of using network device state information for network path selection", Procedia Computer Science, 2018 Publication	2%
2	Stefano Benni, Patrizia Tassinari, Filippo Bonora, Alberto Barbaresi, Daniele Torreggiani. "Efficacy of greenhouse natural ventilation: Environmental monitoring and CFD simulations of a study case", Energy and Buildings, 2016 Publication	1%
3	Grigore Roxana, Popa Sorin, Hazi Aneta, Hazi Gheorghe. "Chapter 16 Study Regarding Numerical Simulation of Counter Flow Plate Heat Exchanger", InTech, 2011 Publication	1%
4	Yulánderson Salguero‐Rodríguez, C. A. Gómez‐Pérez, J. P. Arango Restrepo, Jairo Espinosa. "STATIC MIXER PROPOSAL FOR TUBULAR PHOTOBIOREACTORS TO REDUCE	1%

MIXING ENERGY CONSUMPTION AND ENHANCE LIGHT DARK CYCLES", Journal of Chemical Technology & Biotechnology, 2020
Publication

---

5 "Fluid Mechanics and Fluid Power – Contemporary Research", Springer Science and Business Media LLC, 2017 — 1%
Publication

---

6 "Proceedings of the Fourth International Conference in Ocean Engineering (ICOE2018)", Springer Science and Business Media LLC, 2019 — 1%
Publication

---

7 Md. Mashiur Rahaman, Hafizul Islam, Md. Tariqul Islam, Md. Reaz Hasan Khondoker. "Calm water resistance prediction of a bulk carrier using Reynolds averaged Navier-Stokes based solver", AIP Publishing, 2017 — <1%
Publication

---

8 Geon-Hong Kim, Sanghoon Park. "Development of a numerical simulation tool for efficient and robust prediction of ship resistance", International Journal of Naval Architecture and Ocean Engineering, 2017 — <1%
Publication

---

9 Jialong Jiao, Songxing Huang, Carlos Guedes Soares. "Numerical investigation of ship — <1%

motions in cross waves using CFD", Ocean Engineering, 2021
Publication

---

10 Y.M. Ahmed. "Numerical simulation for the free surface flow around a complex ship hull form at different Froude numbers", Alexandria Engineering Journal, 2011 <1 %
Publication

---

11 "Ship hull form design and optimization based on CFD", Towards Green Marine Technology and Transport, 2015. <1 %
Publication

---

12 Zhi-rong Zhang, Hui Liu, Song-ping Zhu, Feng Zhao. "Application of CFD in ship engineering design practice and ship hydrodynamics", Journal of Hydrodynamics, 2006 <1 %
Publication

---

13 O. Zeitoun. "Numerical Investigation of Natural Convection Around Isothermal Horizontal Rectangular Ducts", Numerical Heat Transfer Part A Applications, 3/1/2006 <1 %
Publication

---

14 Shih-Cheng Hu, Tong Rong Hsiao. "Particle Dynamics in a Front-Opening Unified Pod/Load Port Unit Minienvironment in the Presence of a 300 mm Wafer in Various Positions", Aerosol Science and Technology, 2005 <1 %

Publication

15 Sandra C. K. De Schepper, Geraldine J. Heynderickx, Guy B. Marin. "Modeling the Coke Formation in the Convection Section Tubes of a Steam Cracker", Industrial & Engineering Chemistry Research, 2010 <1%
Publication

16 Grigore Roxana, Popa Sorin, Hazi Aneta, Hazi Gheorghe. "Chapter 16 Study Regarding Numerical Simulation of Counter Flow Plate Heat Exchanger", IntechOpen, 2011 <1%
Publication

17 Mehdi Aslinezhad, Alireza Malekijavan, Peyman Abbasi. "Adaptive neuro-fuzzy modeling of a soft finger-like actuator for cyber-physical industrial systems", The Journal of Supercomputing, 2020 <1%
Publication

18 Tahsin Tezdogan, Atilla Incecik, Osman Turan. "Full-scale unsteady RANS simulations of vertical ship motions in shallow water", Ocean Engineering, 2016 <1%
Publication

19 Manivannan Kandasamy, Seng Keat Ooi, Pablo Carrica, Frederick Stern et al. "CFD validation studies for a high-speed foil-assisted semi-planing catamaran", Journal of Marine Science and Technology, 2011 <1%

Publication

20	Z Ahmad, U.C Kothyari. "Time-line cubic spline interpolation scheme for solution of advection equation", Computers & Fluids, 2001 Publication	<1 %
21	Sunho Park, Se Wan Park, Shin Hyung Rhee, Sang Bong Lee, Jung-Eun Choi, Seon Hyung Kang. "Investigation on the wall function implementation for the prediction of ship resistance", International Journal of Naval Architecture and Ocean Engineering, 2013 Publication	<1 %
22	A Ahmad, C Lopulisa, A M Imran, S Baja. "Soil physicochemical properties to evaluate soil degradation under different land use types in a high rainfall tropical region: A case study from South Sulawesi, Indonesia", IOP Conference Series: Earth and Environmental Science, 2018 Publication	<1 %
23	Hammad Khan, Aitazaz Ahsan, Khawer Ahmed Chauhdhry. "Review of Modern Trend for Numerical Model Testing in Worldwide Towing Tanks", 2019 16th International Bhurban Conference on Applied Sciences and Technology (IBCAST), 2019 Publication	<1 %

24	Bijoy Prasad, Manhar Dhanak. "Hydrodynamics of Advanced-hull Surface Vehicles", OCEANS 2018 MTS/IEEE Charleston, 2018 Publication	<1 %
25	Yavuz Hakan Ozdemir, Ali Dogrul, Boris Barlas, Taner Cosgun. "A NUMERICAL APPLICATION TO PREDICT THE RESISTANCE AND WAVE PATTERN OF KRISO CONTAINER SHIP", Brodogradnja, 2016 Publication	<1 %
26	Ayoung Hwang, Woochan Seok, Sang Bong Lee. "Interaction of turbulences with non-breaking divergent waves in an open channel", International Journal of Naval Architecture and Ocean Engineering, 2021 Publication	<1 %
27	Petr Beneš, Róbert Kollárik. "Preliminary Computational Fluid Dynamics (CFD) Simulation of EIIB Push Barge in Shallow Water", Scientific Proceedings Faculty of Mechanical Engineering STU in Bratislava, 2011 Publication	<1 %
28	Progress in Sustainable Energy Technologies Generating Renewable Energy, 2014. Publication	<1 %

29	Zhang Yongxing, Dong-Joon Kim. "Optimization Approach for a Catamaran Hull Using CAESES and STAR-CCM+", Journal of Ocean Engineering and Technology, 2020 Publication	<1 %
30	"Numerical hydrodynamic optimization of a tanker hull form", Towards Green Marine Technology and Transport, 2015. Publication	<1 %
31	Andrea Farkas, Nastia Degiuli, Ivana Martic. "NUMERICAL SIMULATION OF THE VISCOUS FLOW AROUND A TANKER MODEL", Brodogradnja, 2017 Publication	<1 %
32	Guan Guan, Lei Wang, Jiahong Geng, Zhengmao Zhuang, Qu Yang. "Parametric automatic optimal design of USV hull form with respect to wave resistance and seakeeping", Ocean Engineering, 2021 Publication	<1 %
33	M. Giselle Fernández-Godino, Chanyoung Park, Nam H. Kim, Raphael T. Haftka. "Issues in Deciding Whether to Use Multifidelity Surrogates", AIAA Journal, 2019 Publication	<1 %
34	Yavuz Hakan Ozdemir, Baris Barlas. "Numerical study of ship motions and added	<1 %

resistance in regular incident waves of KVLCC2 model", International Journal of Naval Architecture and Ocean Engineering, 2017
Publication

35 Yi Liu, Lu Zou, Zaojian Zou, Haipeng Guo. "Predictions of ship maneuverability based on virtual captive model tests", Engineering Applications of Computational Fluid Mechanics, 2018 <1%
Publication

36 Ahmed G. Elkafas, Mohamed M. Elgohary, Akram E. Zeid. "Numerical study on the hydrodynamic drag force of a container ship model", Alexandria Engineering Journal, 2019 <1%
Publication

37 Hafizul Islam, Md. Mashiur Rahaman, Hiromichi Akimoto, M. Rafiqul Islam. "Calm Water Resistance Prediction of a Container Ship Using Reynolds Averaged Navier-stokes Based Solver", Procedia Engineering, 2017 <1%
Publication

38 Koushik Mishra, Biplab Ranjan Sarkar, B Bhattacharyya. "Influence of different featured tools on machining accuracy in electrochemical milling", Proceedings of the Institution of Mechanical Engineers, Part B: Journal of Engineering Manufacture, 2019 <1%
Publication

39	Trung-Kien Le, Ngo Van He, Ngo Van Hien, Ngoc-Tam Bui. "Effects of a Bulbous Bow Shape on Added Resistance Acting on the Hull of a Ship in Regular Head Wave", Journal of Marine Science and Engineering, 2021 Publication	<1 %
40	Guo, B.J.. "Seakeeping prediction of KVLCC2 in head waves with RANS", Applied Ocean Research, 201203 Publication	<1 %
41	Multidiscipline Modeling in Materials and Structures, Volume 10, Issue 1 (2014-09-16) Publication	<1 %
42	Nie, Jianhu, Jianfei Wu, Steve Cohen, Blake Carter, and Yitung Chen. "Numerical Simulations of Coupled Flow and Heat Transfer Distributions in a Bipolar Plate of the PEM Electrolysis Cell", Volume 1 Symposia Parts A and B, 2008. Publication	<1 %
43	Nitin Kukreja, Sanjeev Kumar Gupta. "Performance Investigation of Indicated Parameters of a Diesel Blended Engine", IOP Conference Series: Materials Science and Engineering, 2021 Publication	<1 %

44	Nobuaki Sakamoto, Hiroshi Kobayashi, Kunihide Ohashi, Yasutaka Kawanami, Björn Windén, Hikaru Kamiirisa. "An overset RaNS prediction and validation of full scale stern wake for 1,600TEU container ship and 63,000 DWT bulk carrier with an energy saving device", Applied Ocean Research, 2020 Publication	<1 %
45	Shinya ISHIDA, Ken-ichi KAWADA, Yoshitaka FUKANO. "Validation study of SAS4A code for the unprotected loss-of-flow accident in an SFR", Mechanical Engineering Journal, 2020 Publication	<1 %
46	Yao-Hsin Hwang. "SOLUTION OF THE STEADY NAVIER-STOKES EQUATIONS BY THE PRESSURE CORRECTION METHOD IN THE ALE GRID", Numerical Heat Transfer, Part B: Fundamentals, 1993 Publication	<1 %

Exclude quotes	On	Exclude matches	< 5 words
Exclude bibliography	On		